Am J Cancer Res 2021;11(8):3857-3876
www.ajcr.us /ISSN:2156-6976/ajcr0130318

Original Article

3'untranslated regions (3'UTR) of *Gelsolin* mRNA displays anticancer effects in non-small cell lung cancer (NSCLC) cells

Xiaohui Liu[1*], Xiuzhu Huang[1*], Jie Ma[1*], Lu Li[1], Huifan Hu[1], Junxia Feng[2], Xuejuan Gao[1], Yunfang Zhang[2], Langxia Liu[1]

[1]*Key Laboratory of Functional Protein Research of Guangdong Higher Education Institutes and MOE Key Laboratory of Tumor Molecular Biology, Institute of Life and Health Engineering, Jinan University, Guangzhou 510632, China;* [2]*Center of Kidney Disease, Huadu District People's Hospital, Southern Medical University, Guangzhou 510800, Guangdong, China.* [*]*Equal contributors.*

Received January 18, 2021; Accepted June 12, 2021; Epub August 15, 2021; Published August 30, 2021

Abstract: RNA-based therapeutics has attracted substantial interest from both academics and pharmaceutical companies. In this study, we investigated the function and the underlying mechanism of *Gelsolin (GSN)* 3'UTR in NSCLC H1299 and A549 cells. We found that transfected *Flag-GSN* plasmids significantly increased the proliferation, migration and invasion of NSCLC cells, whereas *GSN* 3'UTR could suppress the promotional effect of GSN protein on the development of NSCLC *in vitro.* Interestingly, we observed that these *in vitro* anticancer effects of *GSN* 3'UTR was independent of the co-expression with GSN coding sequence. Moreover, transfected *GSN* 3'UTR affected the actin-cytoskeleton remodeling and epithelial-mesenchymal transition (EMT) processes in H1299 and A549 cells, and targeted the co-expressed proteins to the plasma membrane. Subsequently, RNA pull-down assays have been performed to identify Tra2β protein as a *GSN* 3'UTR binder. We then showed that Tra2β was important for the localized protein expression mediated by *GSN* 3'UTR. Taken together, our results suggested that *GSN* 3'UTR may exert anticancer functions in NSCLC cells through regulating the subcellular localized expression of GSN protein mediated by the interaction between *GSN* 3'UTR-Tra2β.

Keywords: 3'untranslated regions (3'UTR), GSN, Tra2β, non-small cell lung cancer (NSCLC)

Introduction

The utilization of synthetic RNA molecules to alter cellular functions, such as COVID-19 vaccine development based on mRNA technology, is currently out of scope for traditional drug design pipelines and has attracted substantial interest from both academics and pharmaceutical companies [1-3]. Because of the important role of mRNA in gene expression regulation and their high efficiency, safe management, the potential for low-cost production, and capacity for rapid manufacture, mRNA drugs represent promising alternative strategies for the treatment of malignant tumors. Up to now, vaccine platforms against several types of cancer, such as individualized neoepitope mRNA cancer vaccines [4], have presented encouraging results in both animal models and humans [5]. So far, several 3'UTRs in eukaryotic mRNAs have been found to have tumor suppressive activity *in vitro*, capable to cause malignant phenotypic reversion (reduced tumorigenicity) in cultured tumor cells or other malignant cells [6-8]. For example, transfection of *NF-IL6* 3'UTR induced tumor suppression in human hepatoma SMMC7721 cells. Yang *et al.* showed that *FOXO1* 3'UTR inhibited the metastases of breast cancer cells via induction of E-cadherin expression [7]. Hu *et al.* found that the *CCR2* 3'UTR inhibited breast cancer metastasis by repressing EMT *in vitro* and *in vivo* [8]. 3'UTRs exerted biological functions by regulating gene expression, mRNA localization, and competitive binding to miRNA or proteins [9-14]. However, up to date, only a small number of functional 3'UTRs have been characterized and the molecular mechanisms underlying these tumor suppressor effects remain unknown.

Lung cancer is one of the highest morbidity and mortality diseases in the world, and the metastasis is the main cause of death for patients with lung cancer [15, 16]. 85% of lung cancers are NSCLC, which includes lung adenocarcinoma and lung squamous cell carcinoma [17, 18]. Although significant progress has been made in the treatment for patients with advanced epidermal growth factor receptor (EGFR) mutated NSCLC, represented by first line drugs Gefitinib, Erlotinib and Osimertinib, the mortality of NSCLC still remains high, and the important reasons are ascribed to the high cost of drugs, the strong metastasis, unlimited proliferation, and high heterogeneity of lung cancer cells [19-21]. Therefore, it is of great significance to further elucidate the mechanism of pathological progression of NSCLC and identify novel potential efficient and low-cost drugs for the therapy of this cancer.

Gelsolin (GSN) is one of the most abundant actin-binding proteins that mediate cellular motility and play a pivotal role in the pathogenesis of human cancers [22, 23]. However, its functions and regulatory mechanisms in NSCLC have not been fully elucidated. In our previous study, we have been interested in the function of the *GSN* 3'UTR in NSCLC cell *in vitro* [24]. In pursuing our study, we found that the 3'UTR of *GSN* mRNA can reverse the promotional effect of GSN protein on the proliferation, migration, invasion and EMT in H1299 and A549 NSCLC cells, and had a tumor suppressive effect which could be independent of the exogenously co-expressed GSN protein. In this report, we describe these effects and investigate the underlying molecular mechanisms.

Materials and methods

Cell lines and culture

NSCLC cell lines H1299 and A549 were obtained from the Cell Bank of Chinese Academy of Sciences (Shanghai, China). These cells were maintained in high-glucose DMEM medium with 10% fetal bovine serum. All cell lines used in this study was free of mycoplasma contamination.

Plasmids and cloning

The coding sequence (CDS) of human *GSN* (2196 bp), and corresponding *GSN 3*'UTR (240 bp) sequence were amplified from total RNA by RT-PCR. The CDS of *GSN* flanked by BamH I and Xho I restriction sites were inserted into *pCMV-flag* plasmid (*Flag-GSN*). The *GSN* 3'UTR sequence flanked by Xho I and Spe I restriction sites was inserted into *pCMV-flag-GSN*, *pCMV-N-EGFP* or *pCMV-Luc* plasmids to construct the *Flag-GSN-3'UTR*, *EGFP-3'UTR* and *Luc-3'UTR* vectors, respectively. For overexpressing Tra2β, human *Tra2β cDNA* without the 3'UTR was cloned into *pCMV-flag* plasmid (Flag-Tra2β) at BamH I and Xho I sites. All plasmids were sequenced and confirmed for accuracy.

Small interfering RNA transfection

Sequences of siRNA were designed as follows: (si*TRA2β*-1: 5'-AGCUAAAGAACGUGCCAAUTT-3'; si*TRA2β*-2: 5'-CCGAUGUGUCUAUUGUAUATT-3'; si*TRA2β*-3: 5'-ACGCCAACACCAGGAAUUUTT-3'; siNC: 5'-UUCUCCGAACGUGUCACGUTT-3'). Lipofectamine™ 2000 (Invitrogen, CA, USA) was used to transfect cells according to manufacturer's instructions.

mRNA quantification by RT-qPCR

Total RNA of cells was purified and qRT-PCR was performed as previously described. The relative expression level of mRNA was calculated using the $2^{-\Delta\Delta Ct}$ method [25, 26]. The primers were synthesized as follows:

Primer	Forward sequence	Reverse sequence
Vimentin	CCACCAGGTCCGTGTCCTCGT	CGCTGCCCAGGCTGTAGGTG
E-cadherin	TTGCACCGGTCGACAAAGGAC	TGGAGTCCCAGGCGTAGACCAA
N-cadherin	CCCTGCTTCAGGCGTCTGTA	TGCTTGCATAATGCGATTTCACC
Gelsolin	GATCTGGCGTGTGGAGAAGTTCG	CTCTCATCCTGGCTGCACTCATTG
GAPDH	GACAGTCAGCCGCATCTTCT	GCGCCCAATACGACCAAATC

Immunofluorescence (IF) assays

IF assay was performed to confirm the subcellular localization of the indicated proteins as previously described [25]. Appropriate primary antibodies [Gelsolin (11644-2-AP, 1:200), TRA2β (900958001, 1:100)] were used to blot overnight and Alexa Flour 488 or Alexa Fluor 594-conjugated secondary antibody (ZSGB-BIO Co., Ltd., China) was used. F-actin was stained with Rhodamine-phalloidin (Invitrogen™ R415) and the nuclei were stained with DAPI (Beyotime Biotechnology) both for 30 min at room temperature. Cells were captured using Confocal Zeiss LSM 700 equipped with a Zeiss Plan-Neofluar 40 ×/0.75 Oil DIC.

Cell migration and invasion assay

Cell culture inserts (24 well, 8 μm pore size) were used for migration assays and Matrigel-coated chambers (8 μm pore size; BD Biosciences) were used for invasion assays. H1299 and A549 cells (6-8 × 10^4/well) in serum-free DMEM were plated into the upper chamber. Complete medium containing 10% FBS was added to the lower chamber as chemoattractants. After 8-10 h incubation, the migrated or invaded cells were fixed, stained with crystal violet, photographed and quantified in five random fields.

MTT assay

Cells were seeded into 96-well plates at a density of 2 × 10^3 cells/well and cultured overnight. 200 μl working fluid with a final concentration of 5 mg/mL MTT was added to detect cell proliferation at each time-point by measuring the absorbance at 570 nm.

Colony formation assay

Cells were seeded into 6-well plates at a density of 1000/well and then cultured for 2 weeks and stained with crystal violet dye. Clones containing more than 50 cells were counted as one colony.

Western blotting

This assay was performed as described previously [25, 26]. Primary anti-bodies against the following proteins were used: Gelsolin (11644-2-AP; ProteinTech Group), GAPDH (10494-1-AP; ProteinTech Group), E-cadherin (20874-1-AP; ProteinTech Group), Vimentin (10366-1-AP; ProteinTech Group), DDDDK-Tag (66008-3-Ig; ProteinTech Group), β-tubulin (10068-1-AP; ProteinTech Group) and TRA2β (900958001; ABclonal Group).

Biotin pull-down assay

Flag-GSN or *Flag-GSN-3'UTR* PCR fragments containing the T7 RNA polymerase promoter sequence were used as templates to produce the Biotinylated transcripts *in vitro* using T7 RNA polymerase (Invitrogen) and biotin-CTP (Perkin Elmer), and then purified with RNeasy Mini Kit (Qiagen). Biotin pull-down assays were performed by incubating 40 μg of cell lysates with 1 μg of biotinylated transcripts for 30 min at room temperature. The RNA-protein complexes were isolated with streptavidin-coated magnetic beads (Thermo), and the bound proteins were analyzed by Western blotting.

Cell motility video recordings

5 × 10^4 cells/well were seeded into 6-well plates which were then placed on the stage of an inverted microscope equipped with phase-contrast optics, and cultured in a carbon dioxide cell incubator (Sanyo, Japan). A computer-controlled movable stage was mounted on the microscope, allowing simultaneous recordings from several microscopic fields via Cyto-MINI software (Guangzhou Sipu Photoelectric Technology Co. LTD, China). For the observation of cell motility, images of cells were taken sequentially with an interval of 5 min, for a total duration of 20 h.

Statistical analysis

The significance of the data between the two groups were determined by paired Student's t-tests using GraphPad Prism 6 software (GraphPad Software, USA) [27]. Significant differences between multiple groups were analyzed by one-way or two-way analysis of variance (ANOVA). $P < 0.05$ was considered as a significant result.

Results

GSN 3'UTR could suppress the promotional effect of GSN protein on the growth, migration and invasion of NSCLC cells in vitro

To explore the biological function in NSCLC progression of the coding and non-coding 3'UTR sequence in the *GSN* mRNA, we constructed *Flag-GSN* and *Flag-GSN-3'UTR* expression vectors, respectively containing the coding sequence of *GSN* alone or with the 3'UTR at the 3'-end right after the stop codon. H1299 and A549 cells were then either transfected with *Flag-GSN* or *Flag-GSN-3'UTR* plasmid for 24 h, collected and subjected to Western blotting analysis for the verification of GSN overexpression. We found that both H1299 and A549 cells transfected with *Flag-GSN* or *Flag-GSN-3'UTR* vectors displayed higher GSN protein levels than those transfected with control plasmids (Flag-vector) (**Figure 1A** and **1B**). Then,

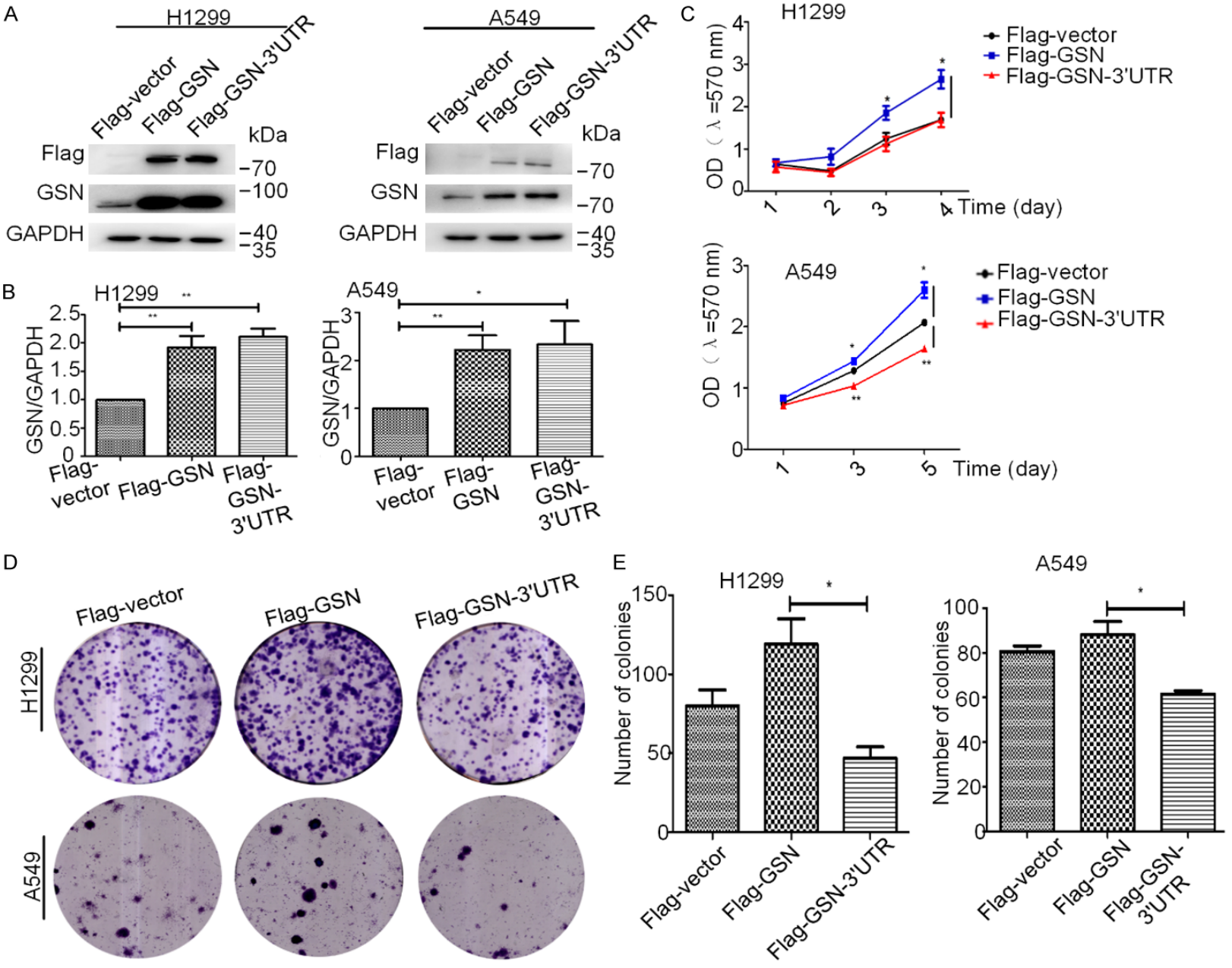
A
H1299
A549
Flag-vector
Flag-GSN
Flag-GSN-3'UTR
kDa
Flag
GSN
GAPDH
-70
-100
-40
-35
B
H1299
A549
GSN/GAPDH
Flag-vector
Flag-GSN
Flag-GSN-3'UTR
C
H1299
A549
OD (λ=570 nm)
Time (day)
Flag-vector
Flag-GSN
Flag-GSN-3'UTR
D
Flag-vector
Flag-GSN
Flag-GSN-3'UTR
H1299
A549
E
H1299
A549
Number of colonies
Flag-vector
Flag-GSN
Flag-GSN-3'UTR

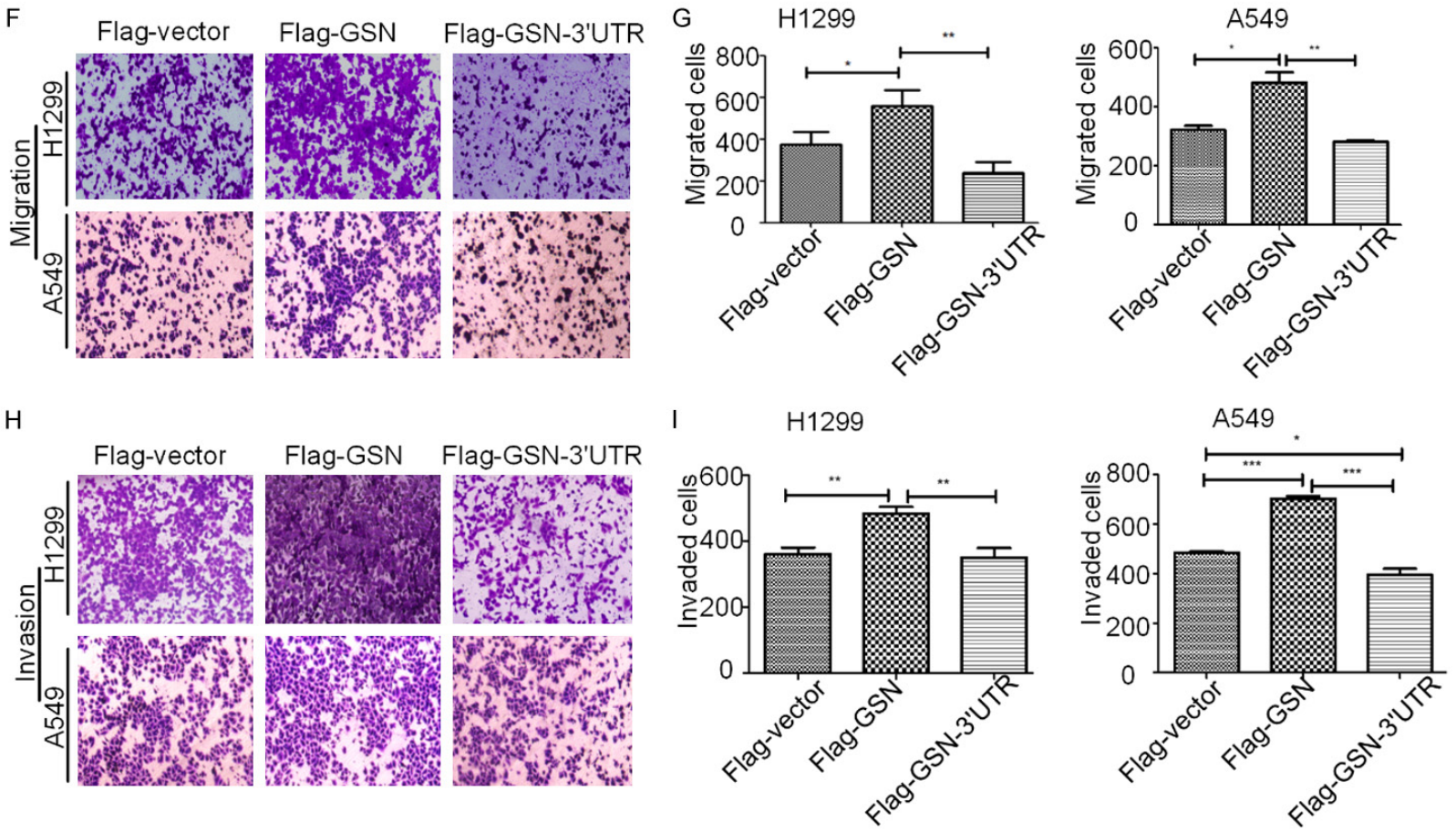

Figure 1. *GSN* 3'UTR could suppress the promotional effect of GSN protein on the growth, migration and invasion of NSCLC cells *in vitro*. H1299 (A) and A549 (B) cells were transfected with *Flag-vector*, *Flag-GSN* and *Flag-GSN-3'UTR* plasmids, and analyzed by western blotting. Signal intensities were quantified with GAPDH as internal control. (C) The effects of *Flag-vector*, *Flag-GSN* and *Flag-GSN-3'UTR* overexpression on the proliferation of H1299 (upper panel) and A549 cells (lower panel), analyzed by MTT assay. (D, E) H1299 and A549 cells were transfected with the indicated plasmids, and the colony formation ability was quantified by a colony formation assay. (F, G) Transwell migration assays of H1299 and A549 cells transfected with the indicated plasmids. (H, I) Transwell invasion assays of H1299 and A549 cells transfected with the indicated plasmids. Data are presented as the mean ± s.d. and are representative of at least three independent experiments. $^{*}P < 0.05$, $^{**}P < 0.01$, $^{***}P < 0.001$.

MTT assay was used to evaluate the cell viability. Our results showed that *Flag-GSN* significantly increased the growth of both H1299 and A549 cells as compared with cells transfected with *Flag*-empty plasmids (**Figure 1C**). Surprisingly, *Flag-GSN-3'UTR* transfected cells displayed similar (for H1299 cells, upper diagram), or less viability (for A549 cells, lower diagram) than control cells, and even lesser than those transfected with *Flag-GSN* plasmids. Colony formation assays were performed to further verify these results. Our results showed that *Flag-GSN* overexpression did not significantly affect the number of colonies of H1299 and A549 cells *in vitro*, although the colony size was bigger with *Flag-GSN* transfected cells than those transfected with empty plasmids. In contrast, overexpression of *Flag-GSN-3'UTR* not only reduced the size of colonies, but also significantly suppressed the ability of H1299 and A549 cells to form colonies *in vitro* as compared with *Flag-GSN* overexpressing cells (**Figure 1D** and **1E**).

Subsequently, we assessed the possible role of the 3'UTR of *GSN* on the migration and invasion abilities of NSCLC cells. Transwell migration and Matrigel invasion experiments were performed with *Flag-GSN* or *Flag-GSN-3'UTR* transfected H1299 and A549 cells as hereinabove. As shown in **Figure 1F-I**, we found that *Flag-GSN* significantly increased the cell migration and invasion in both H1299 and A549 cells. However, overexpression of *Flag-GSN-3'UTR* in H1299 and A549 cells led to a significant decrease in the cell migration (**Figure 1F** and **1G**) and invasion (**Figure 1H** and **1I**) as compared with *Flag-GSN* overexpressing cells, and presenting a level close to that of the control cells.

Taken together, our results indicated that *GSN* 3'UTR exerted opposite effects of exogenic GSN protein on NSCLC cells *in vitro*, reversing the effect of the latter.

Opposite effects of GSN and GSN 3'UTR on EMT process in H1299 and A549 cells

GSN has been reported to function as a switch that controls E- and N-cadherin conversion via Snail in human mammary epithelial cells, and to promote the EMT in hepatocellular carcinoma [28, 29]. To investigate whether the 3'UTR of *GSN* can affect the regulation of EMT by GSN in lung cancer cells, we examined changes in expression levels of key EMT-related markers in H1299 and A549 cells transfected either by *Flag-GSN* or by *Flag-GSN-3'UTR*. The western blot analysis of H1299 cells in **Figure 2A** showed that the downregulation of epithelial marker E-cadherin was observed, concomitant with the upregulation of mesenchymal intermediate filament Vimentin in *Flag-GSN* overexpressing cells, whereas *GSN-3'UTR* weakened the function of GSN protein in promoting the EMT transition. In **Figure 2B**, western blot analysis of A549 cells ascertained the notable increase in the expression of Vimentin in *Flag-GSN* overexpressing cells, and as expected, *Flag-GSN-3'UTR* still counteracted this function. However, for the effects of *Flag-GSN* and *Flag-GSN-3'UTR* on the expression of E-cadherin, quantitative analysis did not lead to a conclusive result, probably due to the technical limitations of Western blotting as a quantitative analysis method (**Figure 2A** and **2B**). Indeed, the mRNA levels of *E-cadherin, N-cadherin, Vimentin* determined by qRT-PCR confirmed the regulation of EMT process by *Flag-GSN* and *Flag-GSN-3'UTR* (**Figure 2C** and **2D**). The mRNA levels of *N-cadherin* and *Vimentin* were both enhanced in H1299 and A549 cells transfected with *Flag-GSN* plasmids, whereas such a promotion of mesenchymal conversion did not occur in H1299 and A549 cells transfected with *Flag-GSN-3'UTR* plasmids. Taken together, these data suggest that the 3'UTR of *GSN* could abrogate the ability of the co-overexpressed GSN protein to promote the EMT process and blocked the cell invasion of NSCLC.

GSN 3'UTR localized the exogenously co-expressed GSN to the membrane

Our results in **Figure 1A** showed that the attachment of the 3'UTR to the CDS of *GSN* did not alter significantly its protein expression level. We then assessed if *GSN* 3'UTR might regulate the localization of its co-expressed GSN protein. By cell immunofluorescence analysis, we noticed that, in contrast to control (empty plasmid-transfected) cells, *Flag-GSN*-overexpressing H1299 cells developed stress fibers across cell body, with Flag-GSN proteins dispersed all over the whole cell body. However, *Flag-GSN-3'UTR* overexpressing H1299 showed more actin-rich short protrusions, with

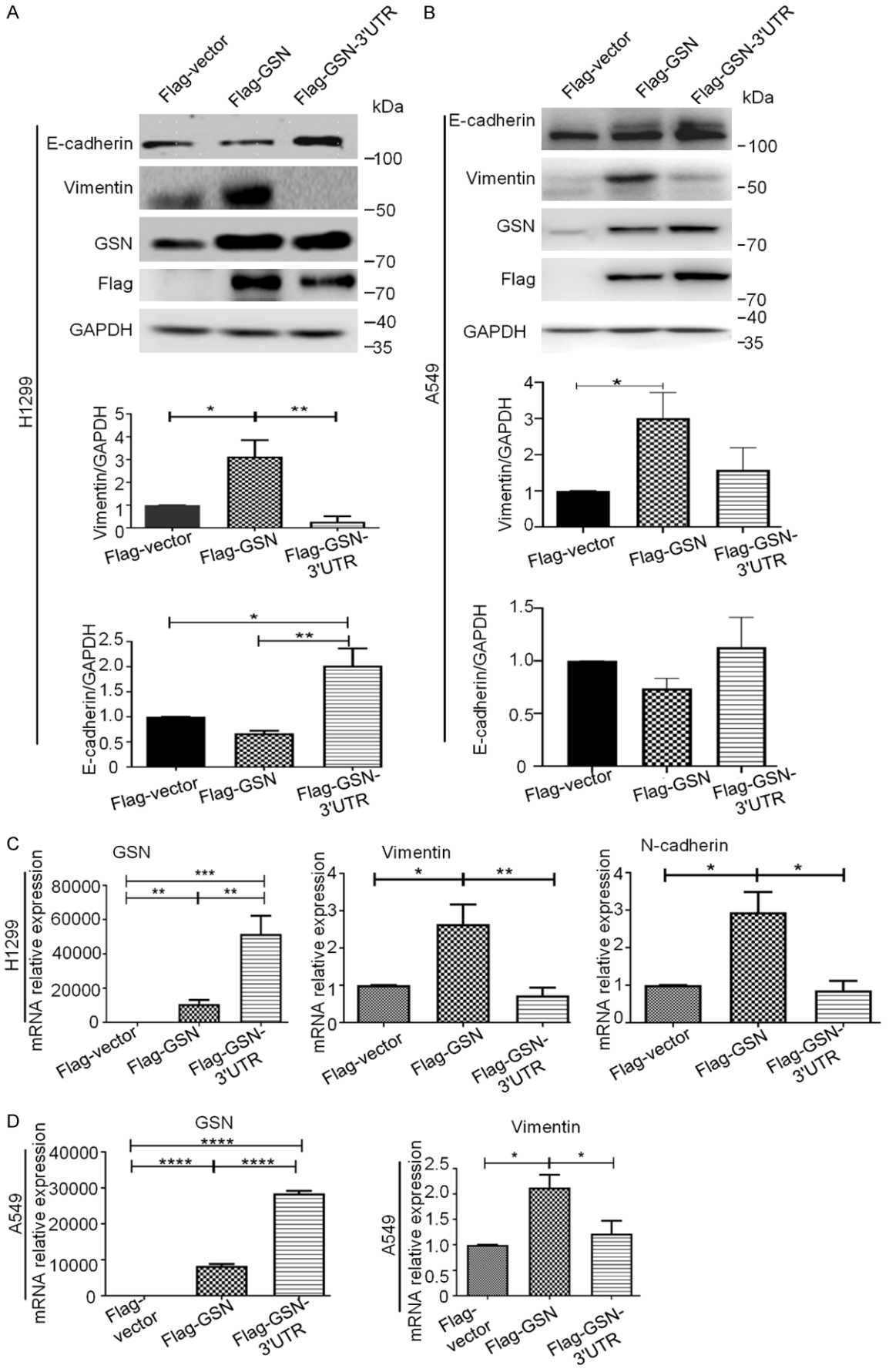
A
Flag-vector
Flag-GSN
Flag-GSN-3'UTR
kDa
E-cadherin
Vimentin
GSN
Flag
GAPDH
H1299
Vimentin/GAPDH
E-cadherin/GAPDH
B
A549
C
GSN
Vimentin
N-cadherin
mRNA relative expression
D

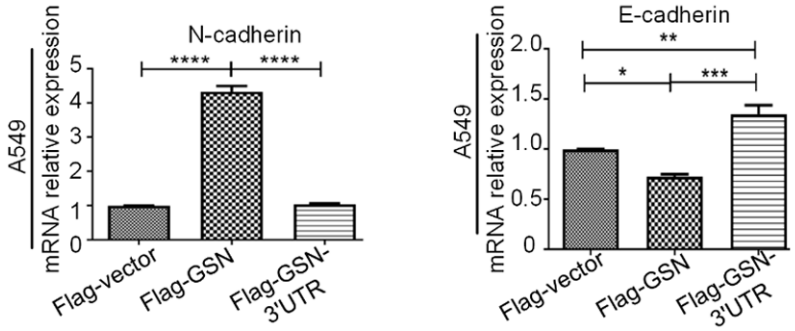

Figure 2. GSN or *GSN* 3'UTR exerted opposite effects on EMT process in H1299 and A549 cells. Protein expression of E-cadherin, Vimentin and transfected Flag-GSN expression by Western blotting in H1299 (A) and A549 (B) cells after transfected with the indicated plasmids. Signal intensities were quantified with GAPDH as internal control. (C, D) The mRNA levels of EMT marker and *GSN* were shown by qRT-PCR after transfected with the indicated plasmids in H1299 (C) and A549 (D) cells. Data are presented as the mean ± s.d. and are representative of at least three independent experiments. $^{*}P < 0.05$, $^{**}P < 0.01$, $^{***}P < 0.001$.

exogenous GSN protein predominately enriched at the plasma membrane, forming a ring-like structure (**Figure 3A** and **3C**). Similarly, *Flag-GSN* and *Flag-GSN-3'UTR* overexpression in A549 cells also resulted in significantly different cytoskeletal actin remodeling, concomitant with different localization of exogenous GSN (**Figure 3B** and **3D**). Taken together, these results suggested that the alterations of GSN subcellular distribution induced by its co-expressed 3'UTR may be directly responsible for determining the regulation of GSN on the proliferation, migration and invasion of H1299 and A549 cells.

The functions of GSN 3'UTR could be independent of the exogenously co-expressed GSN protein

We then addressed whether the functions of *GSN* 3'UTR were dependent of the exogenously co-expressed GSN protein. To this end, we have replaced the co-expressed *GSN* CDS sequence by the *firefly luciferase* CDS sequence. The 3'UTR of *GSN* was inserted right after the stop codon of luciferase CDS in a *pCMV-Luciferase* vector. H1299 and A549 cells transfected with the yielded vector (*Luc-3'UTR*) or the control vector (*Luc-vector*, expressing Luc CDS without *GSN* 3'UTR) were then analyzed by transwell migration, matrigel invasion, and MTT assays. Both H1299 and A549 cells transfected with the *GSN* 3'UTR had a significantly decreased level of cell migration, metastasis, and proliferation in *vitro* (**Figure 4A-E**). These phenotype changes were again associated with the upregulation of E-cadherin expression and the down-regulation of Vimentin and N-cadherin as determined by western blot analysis (**Figure 4F**). Quantitative real-time PCR showed that *GSN* 3'UTR consistently reduced the expression of mesenchymal markers, *N-cadherin*, and *Vimentin* (**Figure 4G**). Together, our data indicated that *GSN* 3'UTR could exert its anticancer functions *in vitro* in a manner independent of the co-expressed GSN protein.

We then asked if *GSN* 3'UTR was also capable to target another protein than GSN to the peripheral region of the cell. To this end, *GSN* 3'UTR were attached to the open reading frame of *enhanced green fluorescence protein* (*EGFP*) and then expressed in H1299 and A549 cells by transfection. Cell immunofluorescence experiments revealed that *GSN* 3'UTR could target the co-expressed EGFP to the proximity of the plasma membrane in co-localization with the F-actin forming a ring-like structure. As commonly observed in previous studies, EGFP protein encoded by *EGFP* CDS in the control cells displayed a diffused pattern of expression (**Figure 5A-D**). This result clearly indicated that *GSN* 3'UTR could target the expression of the upstream CDSs (including that of *GSN* and other genes such as *EGFP*) to the proximity of the plasma membrane.

Transfected GSN 3'UTR disturbed the subcellular localization of endogenous GSN protein in NSCLC cells

During our study, we have observed that endogenous GSN proteins were differently distributed at different cell density in culture. As shown in

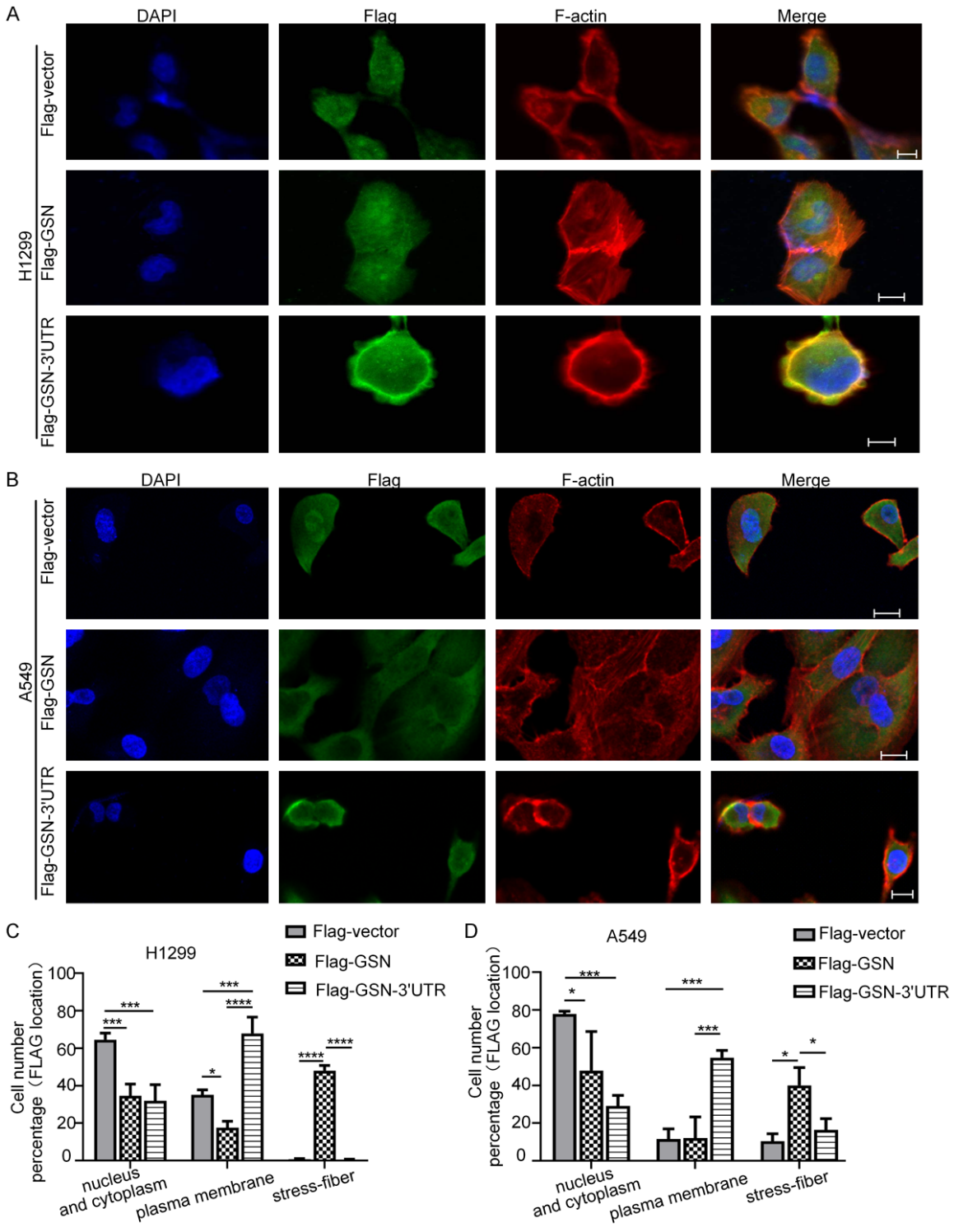

Figure 3. *GSN* 3'UTR localized the exogenously co-expressed GSN to the membrane. Subcellular location of Flag-GSN protein by immunofluorescence confocal microscopy. H1299 (A) and A549 (B) cells transfected with the indicated plasmids were stained with appropriate primary and secondary antibodies. DAPI was used for nuclear staining. F-actin was stained using rhodamine-conjugated phalloidin. Scale bars: 10 μm. (C, D) The counting of cells displaying various Flag-GSN location shown in (A and B). Data shown were from three independent experiments (> 15 cells each, n=3).

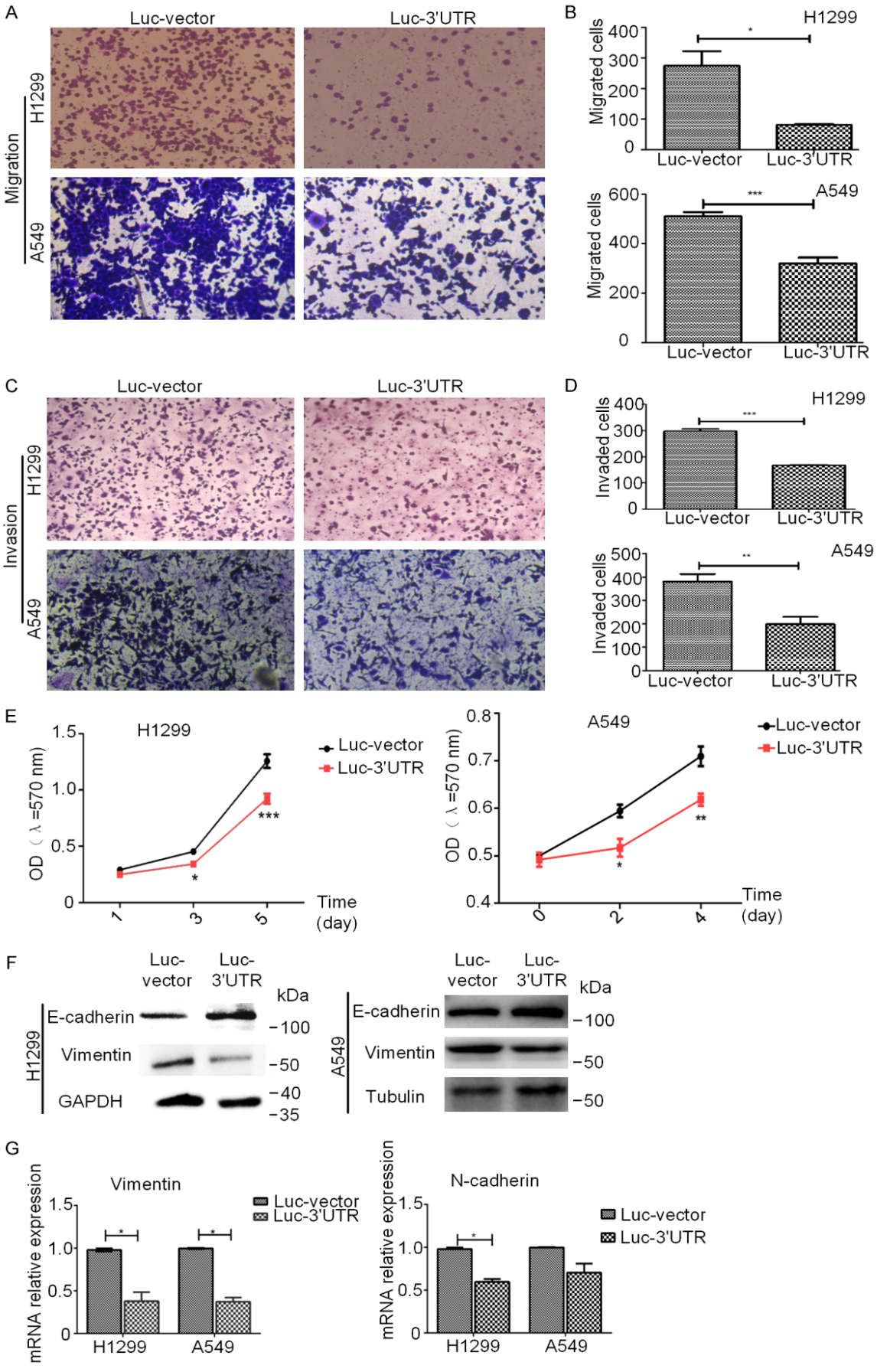
A
Luc-vector
Luc-3'UTR
Migration
H1299
A549
B
H1299
Migrated cells
Luc-vector
Luc-3'UTR
A549
C
Invasion
D
Invaded cells
E
H1299
A549
OD (λ=570 nm)
Time (day)
F
Luc-vector
Luc-3'UTR
kDa
E-cadherin
Vimentin
GAPDH
Tubulin
G
Vimentin
N-cadherin
mRNA relative expression

Figure 4. The functions of *GSN* 3'UTR could be independent of the exogenously co-expressed GSN protein. A, B. Cell migration ability of H1299 and A549 cells transfected with *Luc-vector* or *Luc-3'UTR* was analyzed by transwell assay. C, D. Invasion ability of H1299 and A549 cells transfected with *Luc-vector* or *Luc-3'UTR* was measured by use of transwell assay. E. Transfected of *GSN* 3'UTR in H1299 and A549 cells decreased the proliferation rate by MTT assay. F. The level of E-cadherin, Vimentin and GAPDH was examined by western blotting analysis in H1299 and A549 cells transfected with *Luc*-vector or *Luc-3'UTR*. G. The level of *Vimentin/GAPDH* and *N-cadherin/GAPDH* was examined by RT-qPCR. Data are presented as the mean ± s.d. and are representative of at least three independent EXPERIMENTS. $^{*}P < 0.05$, $^{**}P < 0.01$, $^{***}P < 0.001$.

Figure 5E-H, while a considerable portion of cells expressed GSN proteins at the proximity of the plasma membrane when cells were sparse (at 30% of confluence), in the cells at higher densities (50% and 70% of confluence), GSN protein were expressed in the nucleus and cytoplasm. Moreover, in reminiscence of previous reported findings [30], we have observed that cells *in vitro* culture displayed different mobility at different confluence. In order to demonstrate this observation, we have recorded the motility of cells at different density of culture in the same and also in separated microscopic vision fields during 20 h by taking a photograph per 5 min. In the accelerated (4000 folds) slideshow of these photos, we could observe that cells at low confluence (about 30% of confluence) were less prone to migration than other cells at higher confluence in the surrounding area. However, in the second half of the recording, when cell density became higher, these cells also were subjected to cell division and migration (Supplementary Video 1, cells denoted by curved arrows). This suggests that the plasma membrane localization of endogenous GSN, mainly occurring when the cell density was low, might be related to the decrease in cell motility. Consistently, in *EGFP-vector* transfected H1299 and A549 cells, similarly as observed for EGFP protein, endogenous GSN were evenly distributed throughout the cell body. However, when transfected with *EGFP-3'UTR* plasmid, a large proportion of cells expressed GSN mainly at the cell membrane, in co-localization with EGFP protein (**Figure 5I** and **5J**). These results suggested that the exogenously expressed 3'UTR of *GSN* mRNA could exert its functions through disturbing the subcellular distribution of the endogenous GSN protein.

Tra2β bound to GSN 3'UTR and was important for the localized expression of GSN

It is widely acknowledged that the 3'UTRs are sites for interactions with *trans*-acting effector factors. In order to identify proteins interacting with *GSN* 3'UTR, we have performed an RNA pull-down assay using *in vitro* synthesized *Flag-GSN-3'UTR* transcript with H1299 cell lysates. A total of 66 interacting proteins were then identified using liquid chromatography-mass spectrometry (LC-MS) (Supplementary Figure 1A). 54 of them also bound to *Flag-GSN* (CDS) transcript, thus excluded from further analysis. The remaining 12 3'UTR-specific binders are listed in Supplementary Figure 1B, most of which are reported in the literature as RNA binding proteins. Among these proteins, we were particularly interested by Tra2β (Transformer-2 protein homolog beta).

Tra2β is recognized as a modulator of gene function and associated with cancer. It interacts with RNA targets through its RNA recognition motifs (RRMs) [31, 32]. To directly confirm the association of Tra2β with the 3'UTR of *GSN*, biotinylated transcripts of *Flag-GSN* or *Flag-GSN-3'UTR* was incubated with H1299 cell lysates, the RNA-protein complexes were precipitated with streptavidin-coated beads, and the precipitated Tra2β or α-actin (as a negative control) was examined by western blotting. As shown in **Figure 6A**, biotinylated transcript of *Flag-GSN-3'UTR* specifically interacted with Tra2β, but not with α-actin.

Next, we examined whether Tra2β knockdown affected the localization of GSN. Three specific siRNA against *Tra2β* (si*Tra2β*-1, -2 and -3) were designed and tested as described for their efficiency in H1299 cells (**Figure 6B**). We performed cell immunofluorescence experiments to examine the subcellular distribution of GSN in H1299 cells transfected with si*Tra2β* or siNC. Interestingly, we found that in siNC-treated control cells, endogenous GSN was either located near the plasma membrane or evenly distributed throughout the cell body. However, in Tra2β knockdown cells, endogenous GSN was mainly located in the nucleus (**Figure 6C**). Subsequently, the role of Tra2β in *GSN* 3'UTR-

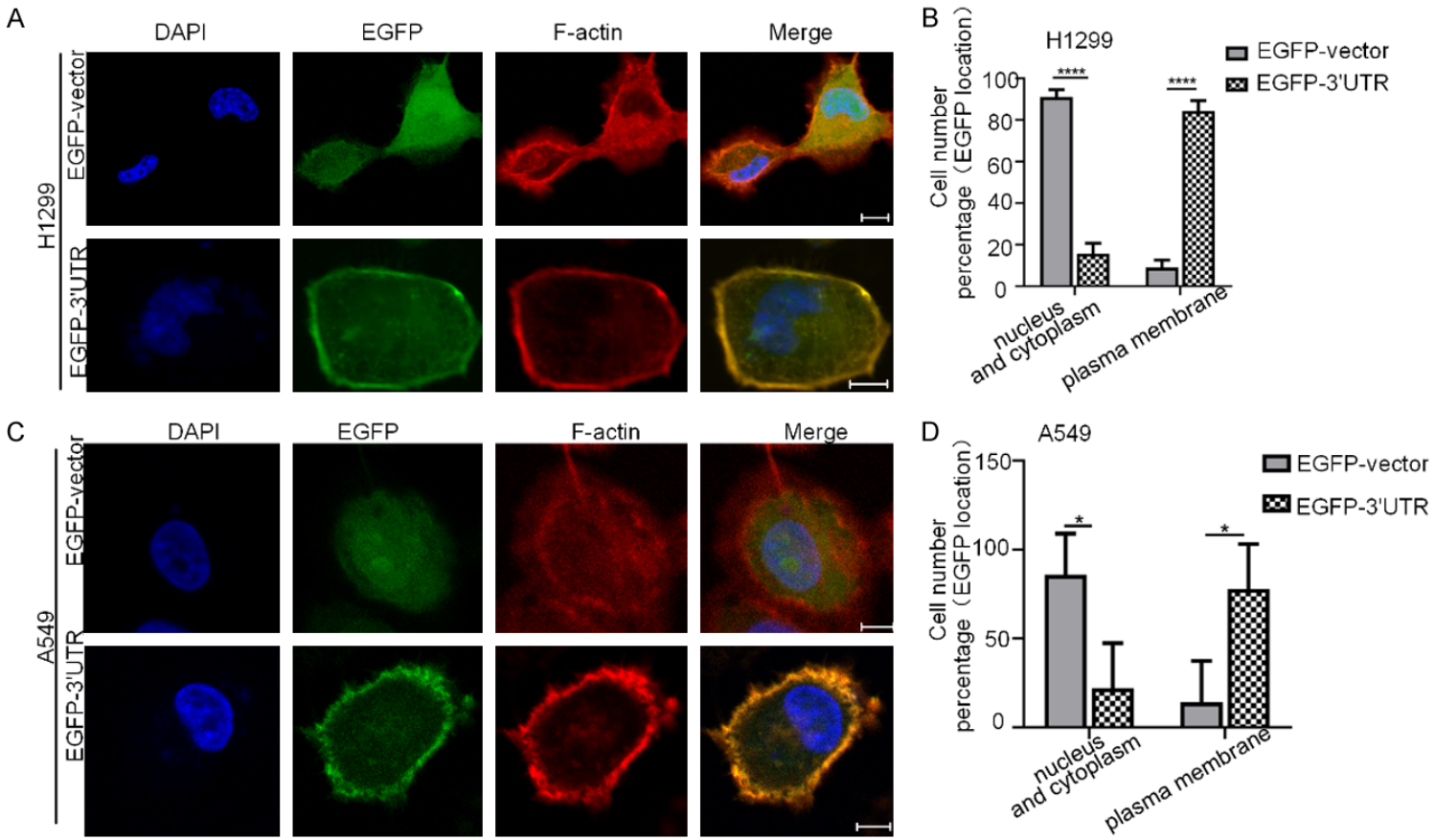
A
DAPI
EGFP
F-actin
Merge
H1299
EGFP-vector
EGFP-3'UTR
B
H1299
EGFP-vector
EGFP-3'UTR
Cell number percentage（EGFP location）
100
80
60
40
20
0
****
****
nucleus and cytoplasm
plasma membrane
C
DAPI
EGFP
F-actin
Merge
A549
EGFP-vector
EGFP-3'UTR
D
A549
EGFP-vector
EGFP-3'UTR
Cell number percentage（EGFP location）
150
100
50
0
*
*
nucleus and cytoplasm
plasma membrane

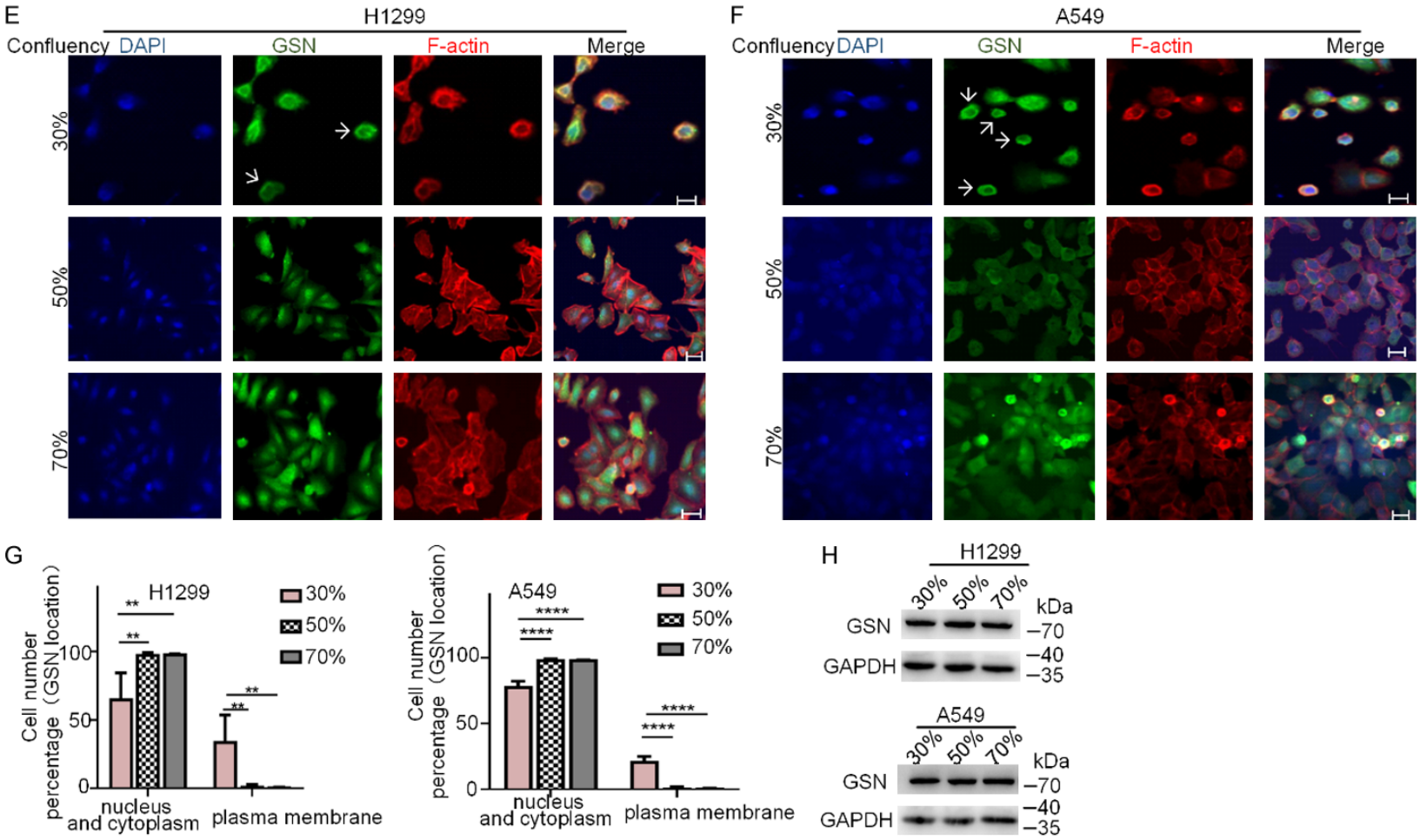
E
H1299
Confluency
DAPI
GSN
F-actin
Merge
30%
50%
70%
F
A549
Confluency
DAPI
GSN
F-actin
Merge
30%
50%
70%
G
H1299
Cell number percentage (GSN location)
100
50
0
**
**
**
**
30%
50%
70%
nucleus and cytoplasm
plasma membrane
A549
Cell number percentage (GSN location)
100
50
0
****
****
****
****
30%
50%
70%
nucleus and cytoplasm
plasma membrane
H
H1299
30%
50%
70%
kDa
GSN
GAPDH
70
40
35
A549
30%
50%
70%
kDa
GSN
GAPDH
70
40
35

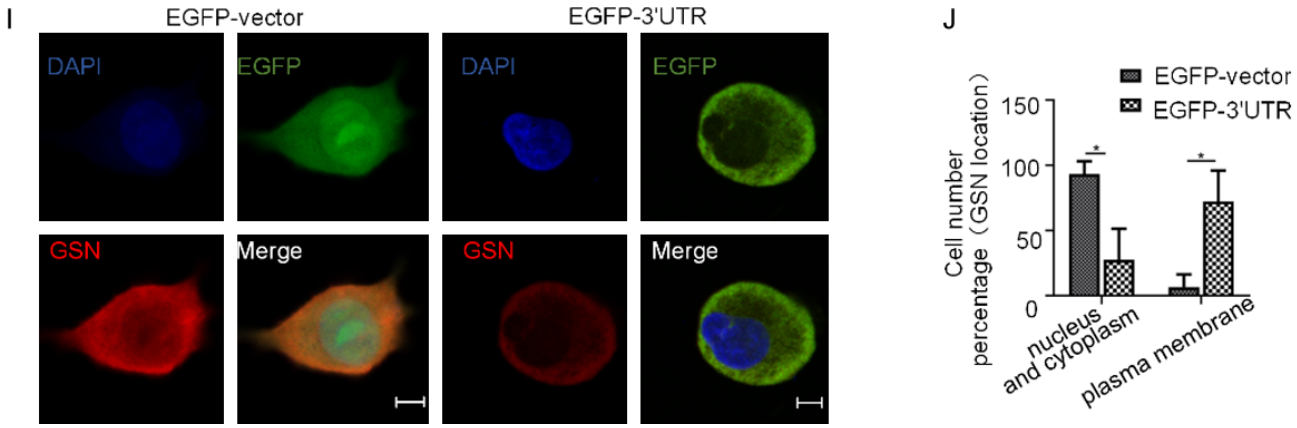

Figure 5. The 3'UTR of *GSN* mRNA is sufficient for the mRNA localization in the proximity of the plasma membrane. (A-D) Immunofluorescence confocal microscopy and corresponding quantification analyses of EGFP subcellular localization in H1299 (A, B) and A549 (C, D) cells transfected with *EGFP-vector* and *EGFP-3'UTR* plasmids. (E-H) Immunofluorescence confocal microscopy and corresponding quantification analyses of endogenous GSN subcellular localization in H1299 (E, F) and A549 (G, H) cells at various confluences. Cells were seeded at 1×10^4 cells/cm^2 and cultured for a total of 24, 48 or 72 h in standard culture medium. At the indicated confluence, cells were fixed and immunolabelled with antibodies for detection of GSN. DAPI was used for nuclear staining. F-actin was stained using rhodamine-conjugated phalloidin. Arrows: endogenous GSN proteins at the proximity of the plasma membrane. (I, J) Immunofluorescence analyses of the localization of transfected EGFP and endogenous GSN proteins in H1299 cells transfected with the indicated plasmids. Quantification analysis was performed based on counting of cells with diverse protein distribution patterns from three independent experiments (> 15 cells each, n=3). Scale bars: 10 μm.

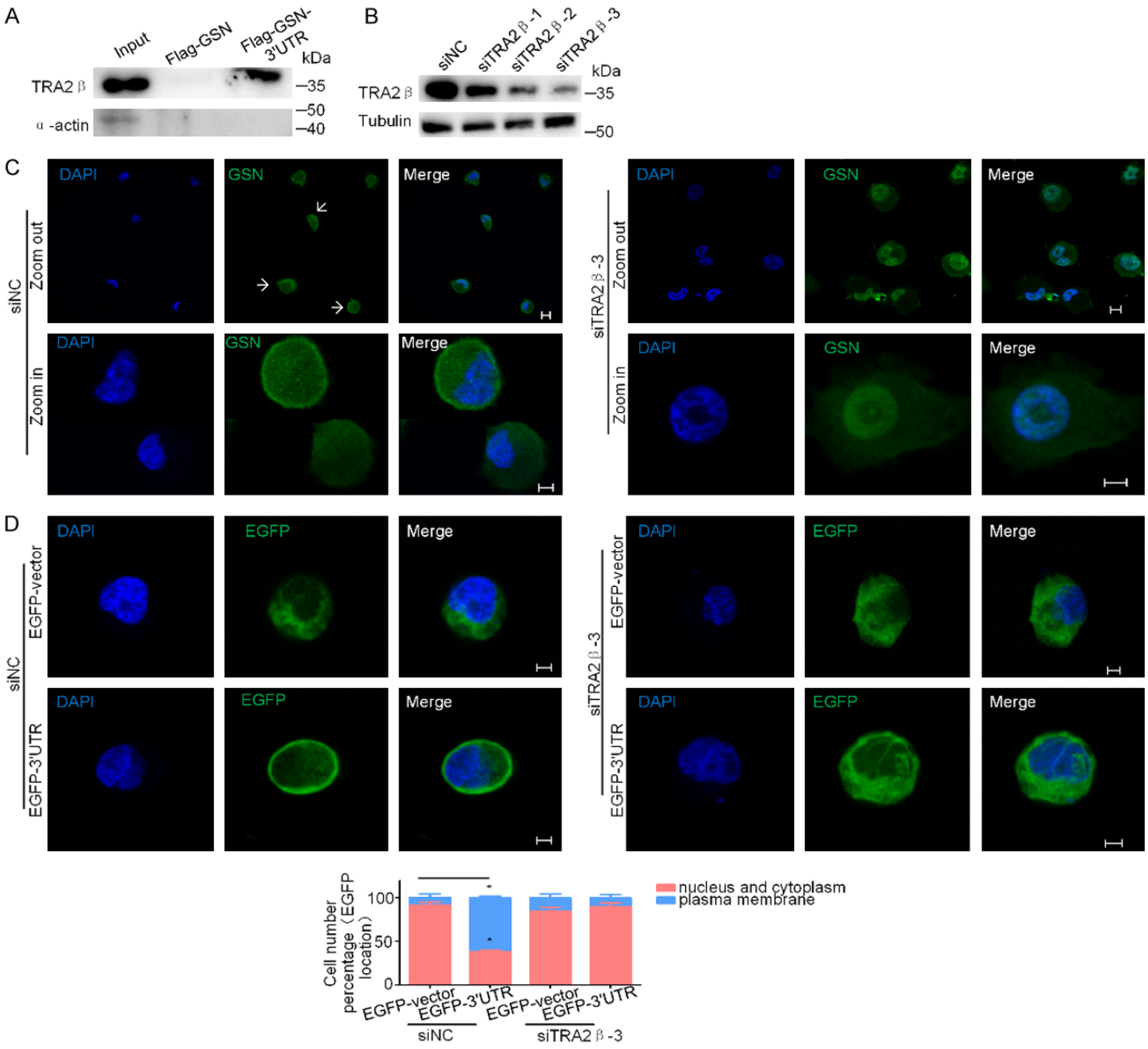
A
Input
Flag-GSN
Flag-GSN-3'UTR
kDa
TRA2 β
–35
–50
α -actin
–40
B
siNC
siTRA2 β -1
siTRA2 β -2
siTRA2 β -3
kDa
TRA2 β
–35
Tubulin
–50
C
siNC
Zoom out
Zoom in
DAPI
GSN
Merge
siTRA2 β -3
D
EGFP-vector
EGFP-3'UTR
EGFP
Cell number percentage (EGFP location)
100
50
0
nucleus and cytoplasm
plasma membrane
siTRA2 β -3

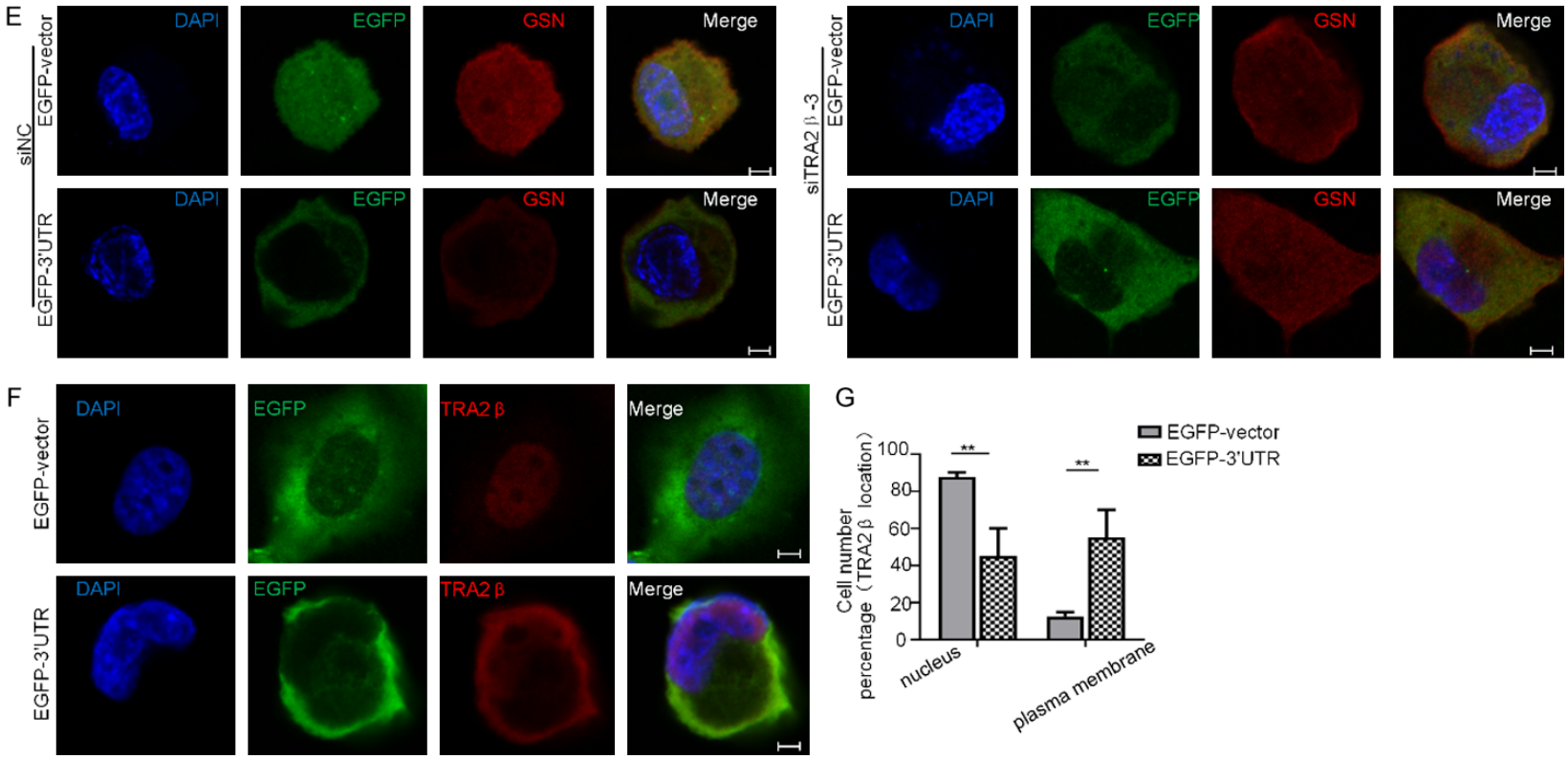

Figure 6. Tra2β bound to *GSN* 3'UTR and was important for the localized expression of GSN. (A) RNA pull-down assay. H1299 cell lysate was incubated with *in vitro* synthesized *Flag-GSN* transcript or *Flag-GSN-3'UTR* transcript as described in Materials and methods. Western blot analysis was performed to detect Tra2β protein bound specifically to GSN 3'UTR. α-actin was used as a negative control. (B) Verification of Tra2β knockdown in H1299 cells using three siRNAs by Western blotting. β-tubulin was used for internal control. (C) H1299 cells were transfected with si*Tra2β*-3 or siNC, and then immunostained with antibodies against GSN (green). Nuclear DNA was stained with DAPI (blue). Arrows: endogenous GSN proteins at the proximity of the plasma membrane. (D, E) H1299 cells were subsequently transfected with siNC or si*Tra2β*-3 for 24 h, and with *EGFP-3'UTR* or *EGFP-vector* for another 24 h, then subjected to immunofluorescence confocal microscopy for the subcellular localization of EGFP (D) or endogenous GSN protein (E). (F, G) Immunofluorescence analyses the subcellular localization of EGFP and endogenous Tra2β protein in H1299 cells transfected with *EGFP-vector* and *EGFP-3'UTR* plasmids. The cell number with each indicated expression pattern was quantified from three independent experiments (> 15 cells each, n=3). Scale bars: 10 μm.

mediated mRNA localization was investigated. H1299 cells were transfected either with specific *Tra2β*-targeting si*RNA* or with siNC for 24 h, and then transfected with *EGFP-3'UTR* or control plasmids for another 24 h. The subcellular localization of EGFP protein was again examined by confocal microscopy. When transfected with *EGFP-3'UTR*, EGFP and endogenous GSN displayed an expected ring-like localization pattern in siNC treated cells, whereas this localization pattern was much less frequently in Tra2β knockdown cells, regardless of whether cells were transfected with *EGFP-3'UTR* or not (**Figure 6D**, **6E** and Supplementary Figure 1C). This phenotype could be reversed through the reconstitution of Tra2β (Supplementary Figure 1D). Re-expression of Tra2β increased the metastatic capacity of Tra2β knockdown cells, in the case of co-transfection with *EGFP-3'UTR* (Supplementary Figure 1E).

Furthermore, as shown in **Figure 6F** and **6G**, Tra2β was mainly localized in the nucleus of EGFP-vector transfected H1299 cells, but in the *EGFP-3'UTR* transfected cells, a large number of Tra2β has been translocated to cytoplasm, precisely in the cell periphery, forming a ring-like structure at the proximity of the plasma membrane. These results suggested that the *GSN* 3'UTR-induced translocation of EGFP protein or endogenous GSN protein was mediated by the interaction between *GSN* 3'UTR and its protein partner Tra2β.

Discussion

GSN expression is downregulated in 60-90% of tumors during carcinogenesis of the breast [33], colon [34], stomach [35], bladder [36], prostate [37], and lung [38]. Literature reported that GSN may be a tumor suppressor that exerts a crucial role in the carcinogenic process [23, 35, 39]. Hiroki *et al.* showed that GSN functions as a switch that controls conversion of cadherin from the E- and N-type, and demonstrated that its knockdown induces EMT in human mammary epithelial MCF10A cells [40]. Conversely, Zhang *et al.* showed that GSN promotes HCC progression by influencing the EMT process [28]. These conflicting observations hinted on the versatile functions and complex regulation mechanisms of GSN. Conceivably, the activities of GSN may be regulated not only by its expression level but also by its subcellular localizations, where different locations elicit different functions. For instance, besides its role in the cytoplasm by severing, capping, nucleating or bundling actin filaments, GSN could also be endowed of unexpected nuclear functions such as transcription regulation [23, 41, 42]. Particularly, the role of the 3'UTR of *GSN* mRNA has not yet been investigated. Meanwhile, during the last decades, there have been studies concerning the association of 3'UTR functions with diverse diseases, including cancer [11, 12, 43, 44]. In our study, when H1299 and A549 cells were transfected with plasmids containing *Flag-GSN* coding sequence, Flag-GSN was uniformly distributed in the cytoplasm, accompanied by the appearance of stress fiber and increased cell migration and invasion. However, the insertion of non-coding 3'UTR sequence in the above expression vector led to the Flag-GSN accumulation at the proximity of the plasma membrane accompanied by distinct changes in actin cytoskeleton and reduced cell growth, migration and invasion (**Figures 1**-**3**). These results suggested that *GSN* 3'UTR might counteract the function of the co-expressed GSN protein to promote cancer development *in vitro*. Interestingly, our further investigation indicated that the effect of *GSN* 3'UTR could be independent of the exogenously co-expressed GSN (**Figure 4**). We found that transfected *GSN* 3'UTR could perturb the localization of endogenous GSN protein. Consistent with this finding, differential localization of GSN was a characteristic associated with different cell confluence of *in vitro* culture, and could be correlated with different cell migration potential (**Figure 5** and Supplementary Video 1).

By using RNA-pull down assay followed by LC-MS, we identified Tra2β as a *GSN* 3'UTR-binder. Knockdown of Tra2β prevented *GSN* 3'UTR-mediated membrane localization of both EGFP and endogenous GSN proteins (**Figure 6** and Supplementary Figure 1). Furthermore, we observed that transfection of *GSN* 3'UTR resulted in the translocation of endogenous Tra2β protein from nucleus to cytoplasm (**Figure 6**). Taken together, all these data converge towards a hypothesis where the transfected *GSN* 3'UTR perturb the subcellular localization of GSN and thereby influence the migration and invasion of NSCLC cell *in vitro* (**Figure 7**). Our findings also point out the possible role of

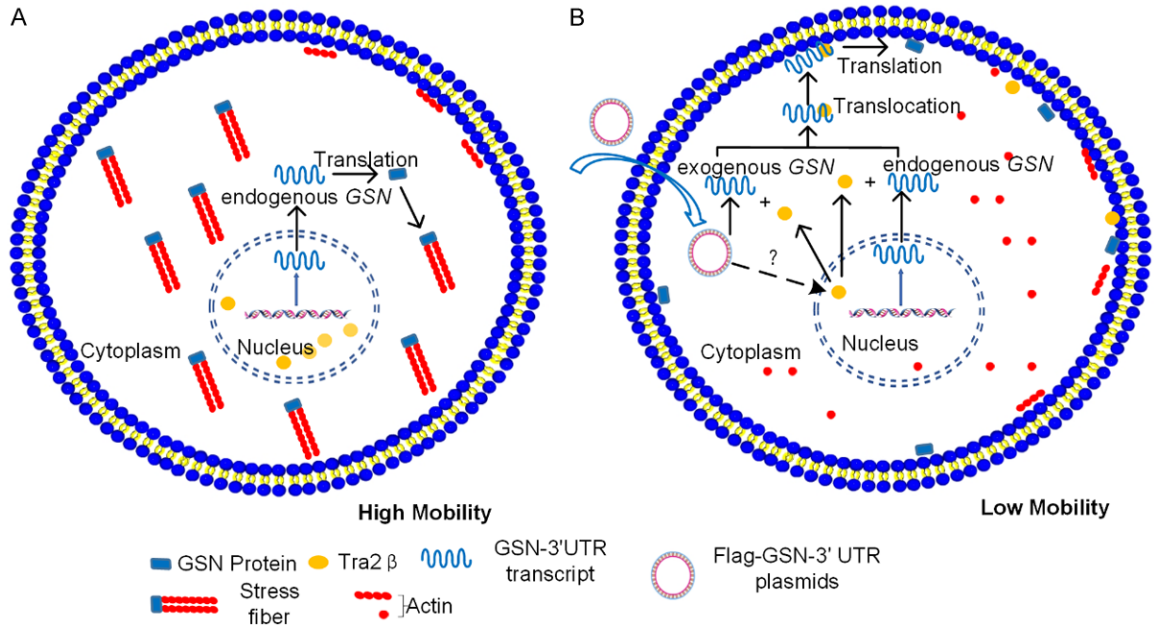

Figure 7. Exogenous *GSN* 3'UTR inhibits the EMT process and migration/invasion abilities of NSCLC cell through interaction with Tra2β and perturbation of endogenous GSN protein localization. A. Without *GSN* 3'UTR transfection, endogenous GSN proteins are distributed in the cytoplasm, Tra2β protein is exclusively located in the nucleus, with actin-rich stress fibers across the cell body, and cells display mesenchymal characteristics with high mobility. B. Upon *GSN* 3'UTR transfection, through an unknown mechanism, Tra2β protein is translocated from the nucleus to the cytoplasm, where it can interact with the endogenous or exogenous *GSN* 3'UTR, bringing the corresponding mRNA to the proximity of the plasma membrane and eliciting the localized translation of the latter. This in turn perturbs the remodeling of actin-rich cytoskeletons, causing disappearance of stress fibers, and inhibits the EMT process, thereby decreases the mobility of the cell.

Tra2β in the mRNA trafficking leading to the localized expression of protein which could influence cancer development. Future investigations would be meaningful to further delineate the precise molecular mechanisms by which the interaction between *GSN* 3'UTR-Tra2β regulates the subcellular localization of GSN protein.

Acknowledgements

This work was supported by the Natural Science Foundation of Guangdong Province (Nos. 2019A1515010182, 2018A030313544), the National Natural Science Foundation of China (No. 81800675), the Guangzhou Science and Technology Project (No. 201804010066).

Disclosure of conflict of interest

None.

Address correspondence to: Drs. Langxia Liu and Xuejuan Gao, Key Laboratory of Functional Protein Research of Guangdong Higher Education Institutes and MOE Key Laboratory of Tumor Molecular Biology, Institute of Life and Health Engineering, Jinan University, Guangzhou 510632, China. Tel: +86-20-85222573; E-mail: langxialiu@gmail.com (LXL); Tel: +86-20-85223139; E-mail: tgaoxj@jnu.edu.cn (XJG); Dr. Yunfang Zhang, Center of Kidney Disease, Huadu District People's Hospital of Guangzhou, Southern Medical University, Guangzhou 510800, China. Tel: +86-13760634557; E-mail: 406112982@qq.com

References

[1] Wang Y, Hoinka J, Liang Y, Adamus T, Swiderski P and Przytycka TM. AptaBlocks: designing RNA complexes and accelerating RNA-based drug delivery systems. Nucleic Acids Res 2018; 46: 8133-8142.

[2] Wang F, Zuroske T and Watts JK. RNA therapeutics on the rise. Nat Rev Drug Discov 2020; 19: 441-442.

[3] L Garner A. RNA-targeted drug discovery: moving beyond promiscuous small-molecule scaffolds. Future Med Chem 2019; 11: 2487-2490.

[4] Türeci Ö, Vormehr M, Diken M, Kreiter S, Huber C and Sahin U. Targeting the heterogeneity of

cancer with individualized neoepitope vaccines. Clin Cancer Res 2016; 22: 1885-1896.
[5] Pardi N, Hogan MJ, Porter FW and Weissman D. mRNA vaccines-a new era in vaccinology. Nature Reviews Drug Discovery 2018; 17: 261-279.
[6] Liu DG, Jiang QH, Wei YY, Sun L, Fu BB, Zhao FK and Zhou Q. Gene expression profile favoring phenotypic reversion: a clue for mechanism of tumor suppression by NF-IL6 3'UTR. Cell Res 2003; 13: 509-514.
[7] Yang J, Li T, Gao C, Lv X, Liu K, Song H, Xing Y and Xi T. FOXO1 3'UTR functions as a ceRNA in repressing the metastases of breast cancer cells via regulating miRNA activity. FEBS Lett 2014; 588: 3218-3224.
[8] Hu J, Li X, Guo X, Guo Q, Xiang C, Zhang Z, Xing Y, Xi T and Zheng L. The CCR2 3'UTR functions as a competing endogenous RNA to inhibit breast cancer metastasis. J Cell Sci 2017; 130: 3399-3413.
[9] Park HJ, Ji P, Kim S, Xia Z, Rodriguez B, Li L, Su J, Chen K, Masamha CP, Baillat D, Fontes-Garfias CR, Shyu AB, Neilson JR, Wagner EJ and Li W. 3'UTR shortening represses tumor-suppressor genes in trans by disrupting ceRNA crosstalk. Nat Genet 2018; 50: 783-789.
[10] Berkovits BD and Mayr C. Alternative 3'UTRs act as scaffolds to regulate membrane protein localization. Nature 2015; 522: 363-367.
[11] Kataoka K, Shiraishi Y, Takeda Y, Sakata S, Matsumoto M, Nagano S, Maeda T, Nagata Y, Kitanaka A, Mizuno S, Tanaka H, Chiba K, Ito S, Watatani Y, Kakiuchi N, Suzuki H, Yoshizato T, Yoshida K, Sanada M, Itonaga H, Imaizumi Y, Totoki Y, Munakata W, Nakamura H, Hama N, Shide K, Kubuki Y, Hidaka T, Kameda T, Masuda K, Minato N, Kashiwase K, Izutsu K, Takaori-Kondo A, Miyazaki Y, Takahashi S, Shibata T, Kawamoto H, Akatsuka Y, Shimoda K, Takeuchi K, Seya T, Miyano S and Ogawa S. Aberrant PD-L1 expression through 3'-UTR disruption in multiple cancers. Nature 2016; 534: 402-406.
[12] Chaudhury A, Hussey GS and Howe PH. 3'-UTR-mediated post-transcriptional regulation of cancer metastasis: beginning at the end. RNA Biol 2011; 8: 595-599.
[13] Mayr C. Regulation by 3'-Untranslated Regions. Annu Rev Genet 2017; 51: 171-194.
[14] Mayr C. What are 3'UTRs doing? Cold Spring Harb Perspect Biol 2019; 11: a034728.
[15] Islami F, Goding Sauer A, Miller KD, Siegel RL, Fedewa SA, Jacobs EJ, McCullough ML, Patel AV, Ma J, Soerjomataram I, Flanders WD, Brawley OW, Gapstur SM and Jemal A. Proportion and number of cancer cases and deaths attributable to potentially modifiable risk factors in the United States. CA Cancer J Clin 2018; 68: 31-54.
[16] Tong L, Shen S, Huang Q, Fu J, Wang T, Pan L, Zhang P, Chen G, Huang T, Li K, Liu Q, Xie S, Yang X, Moses RE, Li X and Li L. Proteasome-dependent degradation of Smad7 is critical for lung cancer metastasis. Cell Death Differ 2020; 27: 1795-1806.
[17] O'Brien TD, Jia P, Caporaso NE, Landi MT and Zhao Z. Weak sharing of genetic association signals in three lung cancer subtypes: evidence at the SNP, gene, regulation, and pathway levels. Genome Med 2018; 10: 16.
[18] Relli V, Trerotola M, Guerra E and Alberti S. Abandoning the notion of non-small cell lung cancer. Trends Mol Med 2019; 25: 585-594.
[19] Leighl NB, Karaseva N, Nakagawa K, Cho BC, Gray JE, Hovey T, Walding A, Rydén A and Novello S. Patient-reported outcomes from FLAURA: Osimertinib versus erlotinib or gefitinib in patients with EGFR-mutated advanced non-small-cell lung cancer. Eur J Cancer 2020; 125: 49-57.
[20] Zhao Y, Liu J, Cai X, Pan Z, Liu J, Yin W, Chen H, Xie Z, Liang H, Wang W, Guo Z, Zhao S, Liang W and He J. Efficacy and safety of first line treatments for patients with advanced epidermal growth factor receptor mutated, non-small cell lung cancer: systematic review and network meta-analysis. BMJ 2019; 367: l5460.
[21] Aguiar PN, Jr, Haaland B, Park W, San Tan P, Del Giglio A and de Lima Lopes G Jr. Cost-effectiveness of osimertinib in the first-line treatment of patients with EGFR-mutated advanced non-small cell lung cancer. JAMA Oncol 2018; 4: 1080-1084.
[22] Feldt J, Schicht M, Garreis F, Welss J, Schneider UW and Paulsen F. Structure, regulation and related diseases of the actin-binding protein gelsolin. Expert Rev Mol Med 2019; 20: e7.
[23] Li GH, Arora PD, Chen Y, McCulloch CA and Liu P. Multifunctional roles of gelsolin in health and diseases. Med Res Rev 2012; 32: 999-1025.
[24] Liu XH, Ma J, Feng JX, Feng Y, Zhang YF and Liu LX. Regulation and related mechanism of GSN mRNA level by hnRNPK in lung adenocarcinoma cells. Biol Chem 2019; 400: 951-963.
[25] Li Z, Liu X, Ma J, Zhang T, Gao X and Liu L. hnRNPK modulates selective quality-control autophagy by downregulating the expression of HDAC6 in 293 cells. Int J Oncol 2018; 53: 2200-2212.
[26] Liu XH, Ma J, Feng JX, Feng Y, Zhang YF and Liu LX. Regulation and related mechanism of GSN mRNA level by hnRNPK in lung adenocarcinoma cells. Biol Chem 2019; 400: 951-963.
[27] Ni J, Hou X, Wang X, Shi Y, Xu L, Zheng X, Liu N, Qiu A and Zhuang S. 3-deazaneplanocin A protects against cisplatin-induced renal tubular

cell apoptosis and acute kidney injury by restoration of E-cadherin expression. Cell Death Dis 2019; 10: 355.

[28] Zhang Y, Luo X, Lin J, Fu S, Feng P, Su H, He X, Liang X, Liu K and Deng W. Gelsolin promotes cancer progression by regulating epithelial-mesenchymal transition in hepatocellular carcinoma and correlates with a poor prognosis. J Oncol 2020; 2020: 1980368.

[29] Tanaka H, Shirkoohi R, Nakagawa K, Qiao H, Fujita H, Okada F, Hamada J, Kuzumaki S, Takimoto M and Kuzumaki N. siRNA gelsolin knockdown induces epithelial-mesenchymal transition with a cadherin switch in human mammary epithelial cells. International Journal of Cancer 2006; 118: 1680-1691.

[30] Hartmann-Petersen R, Walmod PS, Berezin A, Berezin V and Bock E. Individual cell motility studied by time-lapse video recording: influence of experimental conditions. Cytometry 2000; 40: 260-270.

[31] Grellscheid SN, Dalgliesh C, Rozanska A, Grellscheid D, Bourgeois CF, Stévenin J and Elliott DJ. Molecular design of a splicing switch responsive to the RNA binding protein Tra2β. Nucleic Acids Res 2011; 39: 8092-8104.

[32] Best A, Dagliesh C, Ehrmann I, Kheirollahi-Kouhestani M, Tyson-Capper A and Elliott DJ. Expression of Tra2 β in cancer cells as a potential contributory factor to neoplasia and metastasis. Int J Cell Biol 2013; 2013: 843781.

[33] Baig RM, Mahjabeen I, Sabir M, Masood N, Ali K, Malik FA and Kayani MA. Mutational spectrum of gelsolin and its down regulation is associated with breast cancer. Dis Markers 2013; 34: 71-80.

[34] Chen Z, Li K, Yin X, Li H, Li Y, Zhang Q, Wang H and Qiu Y. Lower expression of gelsolin in colon cancer and its diagnostic value in colon cancer patients. J Cancer 2019; 10: 1288-1296.

[35] Wang HC, Chen CW, Yang CL, Tsai IM, Hou YC, Chen CJ and Shan YS. Tumor-associated macrophages promote epigenetic silencing of gelsolin through DNA methyltransferase 1 in gastric cancer cells. Cancer Immunol Res 2017; 5: 885-897.

[36] Kuzumaki N. Progress of research on tumor suppressor genes. Hokkaido Igaku Zasshi 1996; 71: 133-137.

[37] Lee HK, Driscoll D, Asch H, Asch B and Zhang PJ. Downregulated gelsolin expression in hyperplastic and neoplastic lesions of the prostate. Prostate 1999; 40: 14-19.

[38] Kuzumaki N, Tanaka M, Sakai N and Fujita H. Tumor suppressive function of gelsolin. Gan To Kagaku Ryoho 1997; 24: 1436-1441.

[39] Xiao Y, Liu G, Sun Y, Gao Y, Ouyang X, Chang C, Gong L and Yeh S. Targeting the estrogen receptor alpha (ERα)-mediated circ-SMG1.72/miR-141-3p/Gelsolin signaling to better suppress the HCC cell invasion. Oncogene 2020; 39: 2493-2508.

[40] Tanaka H, Shirkoohi R, Nakagawa K, Qiao H, Fujita H, Okada F, Hamada J, Kuzumaki S, Takimoto M and Kuzumaki N. siRNA gelsolin knockdown induces epithelial-mesenchymal transition with a cadherin switch in human mammary epithelial cells. Int J Cancer 2006; 118: 1680-1691.

[41] Kwiatkowski DJ. Functions of gelsolin: motility, signaling, apoptosis, cancer. Curr Opin Cell Biol 1999; 11: 103-108.

[42] Archer SK, Claudianos C and Campbell HD. Evolution of the gelsolin family of actin-binding proteins as novel transcriptional coactivators. Bioessays 2005; 27: 388-396.

[43] Weng J, Han X, Liu K, Yang J, Wei S, Zhang Y, Zeng F, Li Y, Shen L and Gao Y. CD44 3'-untranslated region functions as a competing endogenous RNA to enhance NK sensitivity of liver cancer stem cell by regulating ULBP2 expression. Int J Biol Sci 2019; 15: 1664-1675.

[44] Xiang Y, Ye Y, Lou Y, Yang Y, Cai C, Zhang Z, Mills T, Chen NY, Kim Y, Muge Ozguc F, Diao L, Karmouty-Quintana H, Xia Y, Kellems RE, Chen Z, Blackburn MR, Yoo SH, Shyu AB, Mills GB and Han L. Comprehensive characterization of alternative polyadenylation in human cancer. J Natl Cancer Inst 2018; 110: 379-389.

A

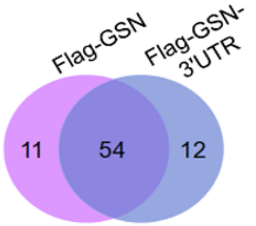

B

Number	Gene Name	Protein IDs	Protein Name
1	RSLIDI	O76021	Ribosomal LI domain-containing protein 1
2	TRA2 β	P62995	Transformer-2 protein homolog beta
3	H1F0	P07305	Histone H1.0
4	THRAP3	Q9Y2W1	Thyroid hormone receptor-associated protein 3
5	KRT8	P05787	Keratin, type II cytoskeletal 8
6	RRBP1	Q9P2E9	Ribosome-binding protein 1
7	RPS3	P23396	40S ribosomal protein 3
8	KRT18	P05783	Keratin, type I cytoskeletal 18
9	SSR3	Q9UNL2	Translocon-associated protein subunit gamma
10	RPS14	P62263	40S ribosomal protein 14
11	H2AFJ	Q9BTM1	Histone H2A.J
12	HIST1H2BM	Q99879	Histone H2B type 1-M

C

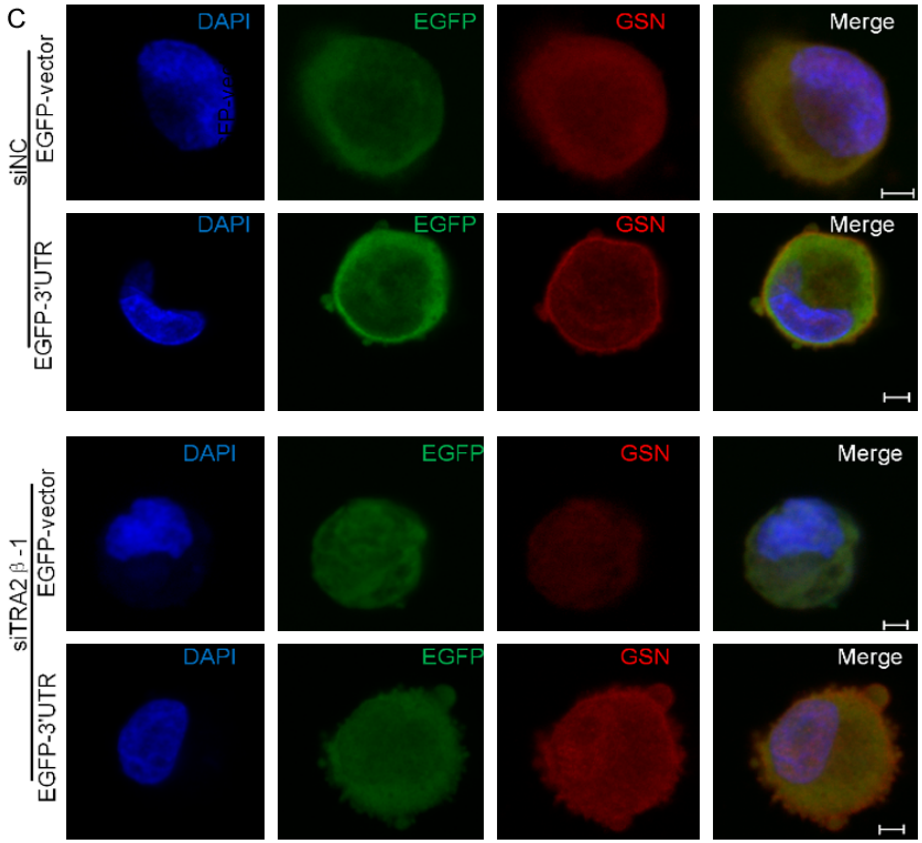

D

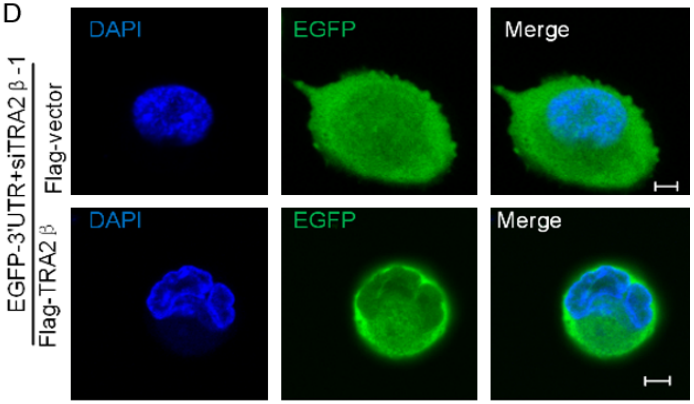

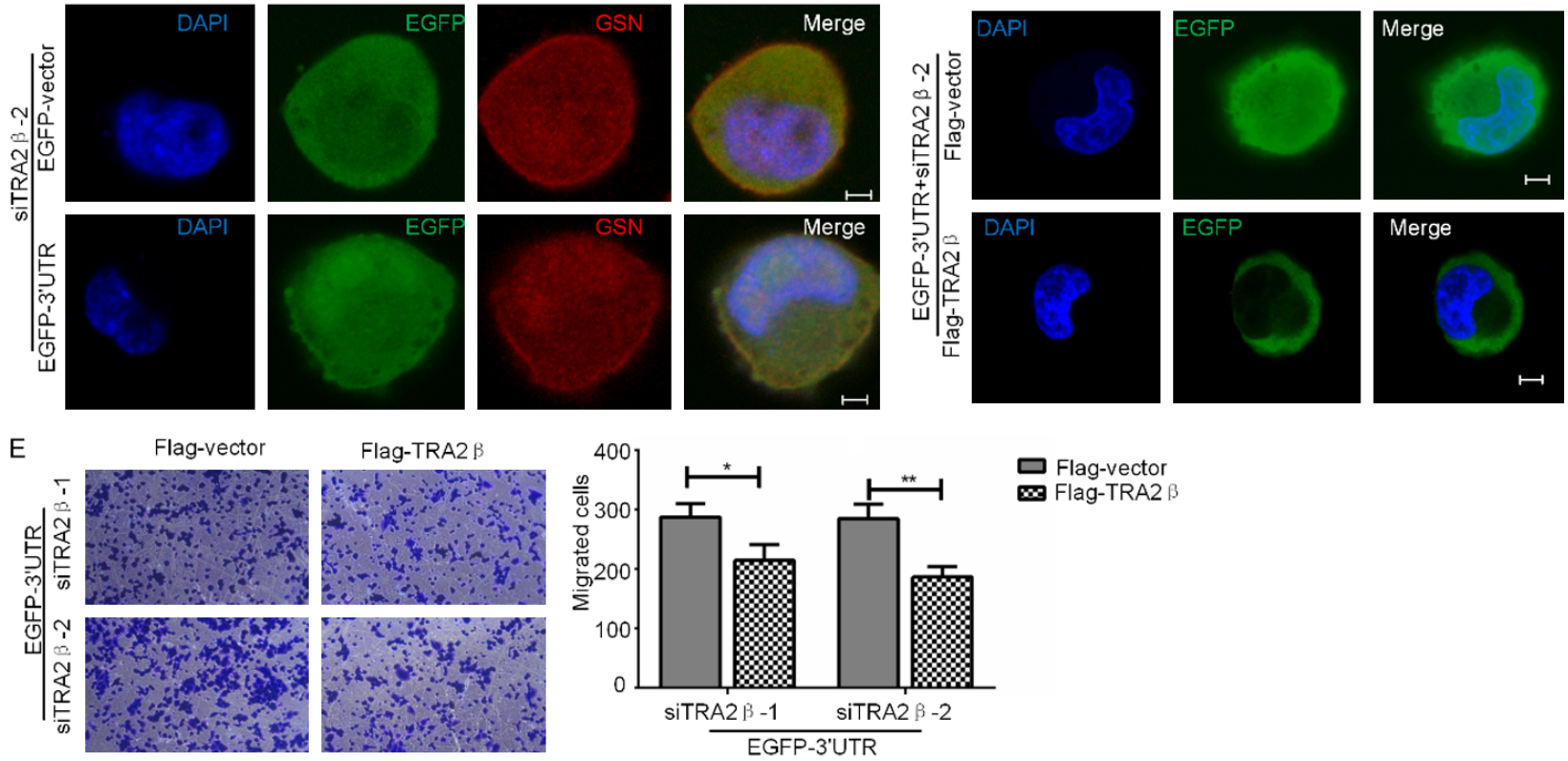

Supplementary Figure 1. (A) The Venn diagram showing the overlap between the proteins bound to *Flag-GSN* transcript and those to *Flag-GSN-3'UTR* transcript. (B) List of 3'UTR region-specific binding proteins. (C) H1299 cells were transfected with siNC or si*Tra2β*-1 or si*Tra2β*-2 for 24 h, and with *EGFP-3'UTR* or *EGFP-vector* for another 24 h, then subjected to immunofluorescence confocal microscopy for the subcellular localization of EGFP. (D, E) H1299 cells were co-transfected with *EGFP-3'UTR and* si*Tra2β*-1 or si*Tra2β*-2 for 24 h, and with *Flag-tagged Tra2β* or with empty vector for another 24 h, then subjected to IF assay (D) or transwell migration assay (E). Scale bars: 10 μm.